

Digital In-line Holographic PIV for 3D Particulate Flow Diagnostics

G. Pan, H. Meng

Abstract We present a digital in-line holographic PIV system for diagnosing 3D particulate flows. This system records in-line holograms directly to a CCD camera and reconstructs them numerically. Since the pixel resolution of CCD cameras is much lower than that of holographic films, conventional particle extraction methods cannot yield high depth resolution that is important for velocity measurement and particulate flow diagnostics. To solve this problem, we have developed a novel particle extraction method based on the complex amplitude of reconstructed wave. With a simple in-line recording setup, this method can reach a depth resolution that is comparable with that of some off-axis holographic PIV systems. This method also alleviates the speckle noise problem intrinsic to in-line particle holography since speckles and particles can be clearly differentiated in complex wavefield. This technique is the basis for a digital in-line holographic PIV (HPIV) system with the addition of Concise Cross Correlation (CCC) and particle pairing algorithm (Pu and Meng 2000). Details of the system hardware and data processing method are described in this paper. The system was tested by both a simulated 3D flow around a collapsing spherical cavity and a laboratory particle suspension.

1

Introduction

Holography is a 3D imaging process that instantaneously captures the volumetric information of a test object. The use of holography for the diagnostics of small particles can be traced back to the 1960's (Thompson 1963, Trolinger et al. 1969). Recent advances in Holographic Particle Image Velocimetry (HPIV) have enabled holographic measurement of particulate flows with particle number densities as high as 30 particles/mm³ in a ~125 cm³ cube with an off-axis system (Pu et al. 2000). While holography is potentially the most powerful tools for diagnosing 3D particulate flows, the conventional procedure of film-based holography, which includes film-based recording, wet chemical processing, and optical reconstruction, have severely restricted the user-friendliness of the holographic imaging technique.

In making holography an easy-to-use technique digital holography is very promising. It records holograms directly to digital media such as CCD sensors and reconstructs the objects numerically. The idea of digital holography was first proposed more than thirty years ago (Goodman and Laurence 1967), and the fundamental theory was established in early 1980's (Yaroslavskii and Merzlyakov 1980). However, practical implementation of digital holography was not feasible until recently when the technologies of digital recording devices and computers have been advanced significantly. Schnars and Juptner were among the first to perform digital holography with a CCD camera (1994). Later on, similar techniques have been applied to various areas including holographic interferometry (Schedin et al. 1999), holographic microscopy (Zhang and Yamahuchi 1998), and biomedical imaging (Boyer et al. 1996).

The application of digital in-line holography to particle measurement was first reported by Adams et al (1997) followed by Nishihara et al. (1997), Kreis et al. (1999) and Murata and Yasuda (2000). In these applications, far-field in-line scattering of 3D particle fields are recorded by a CCD camera, and then reconstructed numerically by calculating the diffraction integral using Fresnel approximation. The 3D position and size of particles are extracted from the intensity images of the reconstructed wave. Based on the same technique, Owen and Zozulya (2000) recently developed a portable digital holographic sensor system for monitoring and characterizing marine particulates. Despite these efforts, digital in-line holography suffers from severe limitations such as extremely low particle loading (only a few particles per hologram) and extremely poor depth resolution (about several hundred microns for particles a few microns in diameter). Similar problems exist for conventional in-line holography, and previous studies have shown that they are caused by the intrinsic speckle noise of in-line holography (Meng et al. 1993) and the small effective aperture of forward light scattering (Meng and Hussain 1995), respectively. However, these problems are much more severe with digital holography than with its optical counterpart since the pixel resolutions of CCD sensor are lower by an order of magnitude than that of holographic films.

In this paper, we present a novel technique for particle measurement using digital in-line holography. This technique uses a simple in-line recording setup and a convolution-based numerical reconstruction scheme, where particle extraction is based on the complex amplitude of reconstructed wave instead of just image intensities. With

this new technique, particle depth resolution is drastically improved and the speckle noise problem common to in-line particle holography is alleviated. This system can also measure particle velocities with the addition of Concise Cross Correlation (CCC) and particle pairing algorithm proposed by Pu and Meng (2000).

2 System design

Fig. 1 shows the hardware components of the digital in-line holography system. The whole setup is quite simple, requiring only one collimated laser beam for generating both object wave and reference wave. In-line holograms of particles are directly recorded by a CCD camera and then transferred to a computer for numerical reconstruction and particle extraction. A diode laser source and a low-end CCD camera will work for this system. However, we chose to use a 532nm Nd:YAG laser (Newwave PIV laser) and a 12-bit cooled CCD camera (PCO Sensicam, 1280×1024 pixels, 6.7 μm pixel size) in consideration of further extension to 90° light scattering and full-scale velocity measurement.

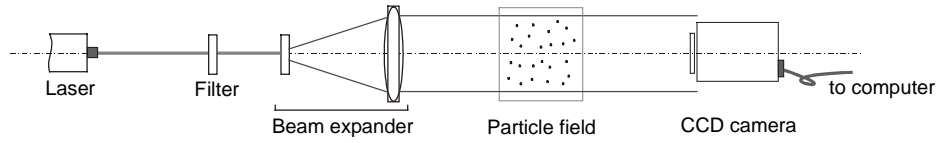


Fig. 1. Hardware setup of digital in-line HPIV system

Fig. 2 is the flow chart of the data processing software. First the digital holograms are reconstructed plane by plane at different z positions (see Fig. 3) to get the wave that consists of virtual and real image waves of all particles in the volume. Then the intensity images of the reconstructed wave are generated on each plane to extract objects, which could be either particle images or speckle noises. The size and x - y position of these objects are obtained by segmenting these images. After this, the complex amplitude of the reconstructed wave in the area occupied by these objects is processed to identify particles and extract their z position. Finally, two sets of particle 3D positions obtained from two consecutive (double-exposure) holograms are processed using the concise cross-correlation (CCC) and particle pairing method (Pu and Meng 2000) to get particle 3D velocity.

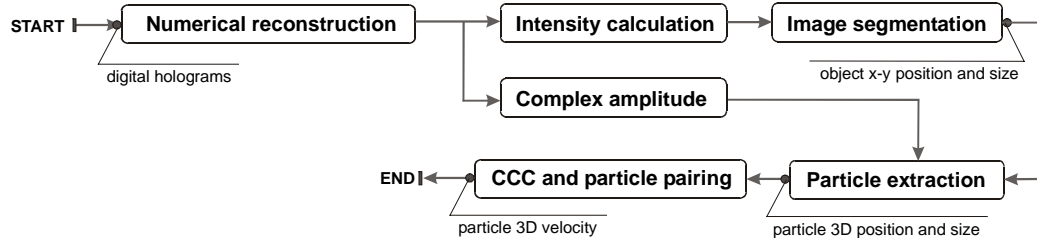


Fig. 2. Flow chart of data processing in digital in-line HPIV system

3 Numerical reconstruction

In a typical setup of in-line particle holography, as the one used in this system, a coherent plane wave propagates through the particle field. The light scattered by particles serves as the object wave and the unscattered light serves as the reference wave. The interference between these two waves is recorded onto the recording media and produces a hologram. In the reconstruction stage the same plane wave is diffracted, usually optically but here numerically, by the hologram. (see Fig. 3). Since the object size is sufficiently small in particle holography, the diffracted wave can be calculated using Fresnel-Kirchhoff integral:

$$U(x, y, z) = \iint I_H(\xi, \eta) \cdot \frac{\exp(jkz)}{j\lambda z} \cdot \exp\left\{\frac{jk}{2z}[(x-\xi)^2 + (y-\eta)^2]\right\} d\xi \cdot d\eta, \quad (1)$$

where I_H is the intensity of hologram, λ is the wavelength of coherent light wave, and $k=2\pi/\lambda$.

Eq. 1 can be written as a 2D convolution, $U(x, y, z) = I_H(\xi, \eta) \otimes h_z(x, y)$, where h_z is the convolution kernel:

$$h_z(x, y) = \frac{\exp(jkz)}{jkz} \exp\left\{\frac{jk}{2z}(x^2 + y^2)\right\}. \quad (2)$$

Based on the convolution formula, the implementation of numerical reconstruction is straightforward and can be carried out efficiently by fast Fourier transform (Onural and Scott 1987). Since the Fourier transform of h_z is known analytically, only one inverse Fourier transform is needed on each reconstruction plane.

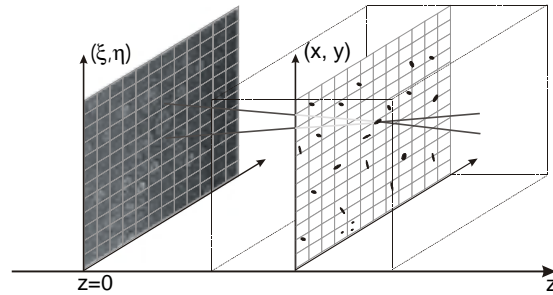


Fig. 3. Coordinate system in numerical reconstruction

Fig. 4 shows an example of numerical reconstruction of a digital hologram of $50\ \mu\text{m}$ particles. The pixel size of the CCD sensor is $6.7\ \mu\text{m}$, which gives a recording resolution of 75 lp/mm (lp: line pairs). The hologram is pre-processed by local mean subtraction to eliminate the effect of non-uniform illumination. In the numerical reconstruction, the directly transmitted wave is removed by filtering out the zero-frequency component in the Fourier domain. This also suppresses the speckle noise since interference of the directly transmitted wave with the virtual image wave is the major source of the noise when particle concentration is low (Meng and Hussain 1995).

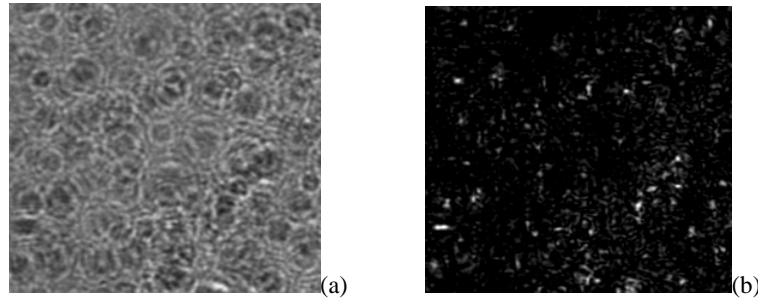


Fig. 4. Example of numerical reconstruction. (a) Digitally recorded hologram of $50\ \mu\text{m}$ particles. (b) Intensity image of reconstructed wave at $z=40\ \text{mm}$.

4 Particle extraction

In holographic PIV aiming at diagnosing particulate flows, particles, represented by their 3D position and size, need to be extracted from the particle holograms. Conventional approaches of particle extraction, which rely on optical reconstruction, uses only intensity images of the reconstructed wave since it is highly difficult to record complex amplitude. Although such intensity-based methods can provide x and y positions of particles accurately, they usually have trouble in obtaining the precise z positions because of the large depth of focus of particle images. In the reconstruction of in-line particle holograms it is common to observe cigar-shaped particle images, often longer than 1mm. Even with off-axis holography and 90° light scattering, the depth of focus of particle images can still be greater than $200\ \mu\text{m}$ (Pu et al. 2000). This problem is more serious in digital holography because only low-frequency fringes could be recorded with the limited pixel resolution of CCD cameras. With a typical $1\text{K}\times 1\text{K}$ CCD camera of today's technology, the pixel size is in the range of $6\sim 10\ \mu\text{m}$, which translates to a resolution less than 100 lp/mm, compared with 5000 lp/mm of holographic film plate. Therefore, in digital holographic PIV intensity-based methods cannot give accurate particle positions, which are indispensable for HPIV and particulate flow studies. To solve this problem, we have developed a new particle extraction method for digital holography, which uses complex amplitude of the reconstructed wave instead of only intensity images.

In hologram reconstruction, the reconstructed wave U can be composed of four terms: the real image wave U_1 , the virtual image wave U_2 , the directly transmitted wave U_3 , and the autocorrelation of the object wave U_4 . The U_4 component is rather weak in particle holography and can be neglected. U_3 component can be easily filtered out in numerical reconstruction. Consequently, the calculated wavefield U can be written as

$$U = U_1 + U_2 = \sum_i r_i + \sum_i v_i, \quad (3)$$

where r_i and v_i are the real and virtual image wave of particle i , respectively.

Suppose a particle k is originally located at $(x_k, y_k, -z_k)$ during the recording phase, its reconstructed real image wave r_k will converge at the point (x_k, y_k, z_k) on the opposite side of the hologram (see Fig. 3). At this point the imaginary part of r_k vanishes. As a result, the imaginary part of U , which is

$$\text{Im}(U) = \text{Im}(r_k) + \text{Im}\left(\sum_{i \neq k} r_i + \sum_i v_i\right), \quad (4)$$

becomes

$$\text{Im}(U) = \text{Im}(\Omega), \text{ where } \Omega = \sum_{i \neq k} r_i + \sum_i v_i \quad (5)$$

It can be proven (Pan and Meng 2001) that, in the cigar-shape region occupied by the image of particle k , the variances of $\text{Im}(U)$ on different x - y planes has the minimum at $z=z_k$, and the minimum value equals to the variance of $\text{Im}(\Omega)$ on that plane. Therefore, particle z positions can be extracted by examining the variances of $\text{Im}(U)$ on the planes at which the particle images reside.

On the other hand, since r_k converges when $z < z_k$ and then diverges when $z > z_k$, $\text{Im}(r_k)$ changes from negative to positive (or the other way) with a cross-zero point at z_k . $\text{Im}(U)$ has similar characteristics as those of $\text{Im}(r_k)$ in the region near particle k , except that the cross-zero point is not exactly at (but close to) z_k due to the addition of $\text{Im}(\Omega)$. However, speckles, though usually indistinguishable from particles in intensity images (e.g., in Fig. 4(b)), do not enjoy such characteristic. Therefore, the variation pattern of $\text{Im}(U)$ along the z direction can be used to differentiate particles from speckles.

Fig. 5 shows the variance and mean of $\text{Im}(U)$ in the region near a 20μ particle. The data is obtained from the numerical reconstruction of a synthesized hologram of a random particle field, of which the particle positions and sizes are known. Prior to the reconstruction, the hologram is processed by local-mean subtraction and low-pass filtering. As shown in Fig. 5, the variance of $\text{Im}(U)$ is minimum at $z=36,040 \mu\text{m}$, compared with the known $z_k=36,027 \mu\text{m}$. Also shown in this figure is the intensity of U ($|U|^2$) near z_k . Evidently, the intensity is almost constant over a large range of z . Hence intensity-based methods fail to provide accurate z . Fig. 5 also demonstrates the variation pattern of the mean value of $\text{Im}(U)$, which changes from positive to negative in the region near the particle in-focus position.

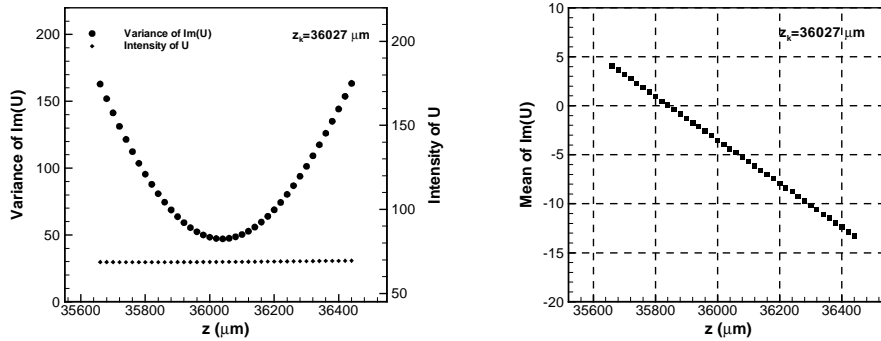


Fig. 5. Variance (left) and mean value (right) of $\text{Im}(U)$ in the region near a particle

In this digital in-line holographic PIV technique, particles' x - y position and size are extracted directly from intensity images prior to applying the complex amplitude method. A segmentation method is used to extract objects from the intensity image on each scanning plane. Since the peak value of intensity varies from plane to plane, thresholds for image binarization are selected based on the histogram of each plane.

5 Velocity extraction

Particle velocities can be calculated using particle position data extracted from two consecutive (double-exposure) holograms. In this system, the Concise Cross Correlation (CCC) and particle pairing algorithm is the key to the velocity extraction. This algorithm, proposed by Pu and Meng (2000), takes two corresponding groups of particle positions, keeps one of them fixed in its original place, and then translates the other one in the 3D space and computes their correlation intensity. The shift yielding the highest correlation peak is considered the mean displacement of the particle group. After the mean displacement of the particle group is determined, individual particles are paired and the velocity of each particle is obtained.

6

Results

(a) Application to a simulated 3D flow

To check the accuracy of numerical reconstruction and particle extraction method described above, the system was first tested by a simulated irrotational flow around a collapsing spherical cavity. This flow is three-dimensional in Cartesian coordinate and the velocity vector can be written as (Lighthill 1986)

$$\vec{V} = \nabla \phi, \phi = -\frac{a^2}{r} U_a, \quad (6)$$

where r is the distance to the center of the cavity, a is the cavity's radius and U_a is the cavity's collapsing rate.

In the simulation, tracer particles ($d_p=20 \mu\text{m}$) were randomly seeded in a $4 \times 4 \times 5 \text{ mm}^3$ region that is outside a spherical cavity of 2mm in radius. The particles were then shifted to the next positions according to the known 3D velocity distribution. Two-frame, double-exposure in-line holograms were calculated using the Fresnel-Kirchhoff integral given by Eq. 1, in which I_H was replaced by a circ function that models particles' amplitude transmittance function. Fig. 6 shows the simulated double-exposure hologram. In this hologram, the particle seeding density, n_s , is 2.6 mm^{-3} .

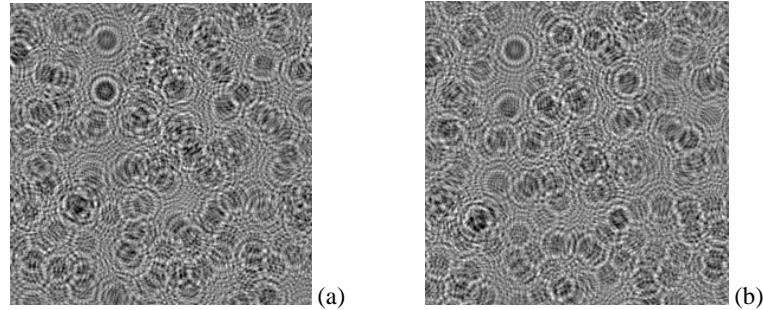


Fig. 6. Simulated double-exposure hologram of $20 \mu\text{m}$ tracer particles. (a) and (b) are the first and the second exposure, respectively. The seeding density is 2.6 mm^{-3} and the viewing volume is $4 \times 4 \times 5 \text{ mm}^3$.

The accuracy of particle extraction, particularly the particle z position, was checked by simulated holograms at different seeding densities. The extracted particle z positions were compared with the known particle positions to evaluate the errors δ_z . Fig. 7 shows the cumulative distribution functions (CDF) of δ_z at three seeding densities, $n_s=1.5, 2.6$ and 6.1 mm^{-3} respectively. Clearly the mean and median value of δ_z increases with n_s . It is found that the minimum-variance detection procedure in particle extraction is sensitive to the fluctuation of $\text{Var}(\text{Im}(\Omega))$ along the z direction. In reconstruction when the noise contributed by the out-of-focus particles increases, this fluctuation becomes more prominent, so that the accuracy of minimum-variance detection is affected.

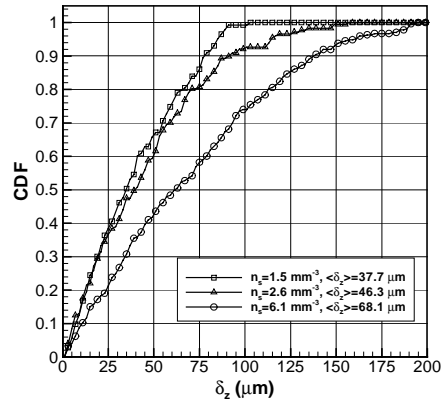


Fig. 7. Cumulative distribution function (CDF) of error δ_z at three particle seeding densities.

Using particle 3D positions as the input, particle velocities were calculated by Concise Cross-correlation (CCC) and particle pairing method (Pu and Meng, 2000). The velocities of scattered particles were also mapped onto a uniform grid by interpolation. Since tracer particles were assumed to follow the flow, the flow velocity field was measured. Fig. 8(a) shows the 3D vector map of the flow, of which the fluid moves toward the center of cavity located at the origin. To compare the HPIV data with the known velocity given by Eq. (6), the measured velocities were converted from Cartesian coordinate to spherical coordinate, in which the flow becomes one-dimensional. Fig. 8(b) shows the radial velocity V_r as a function of radial distance r . Overall the HPIV data is reliable.

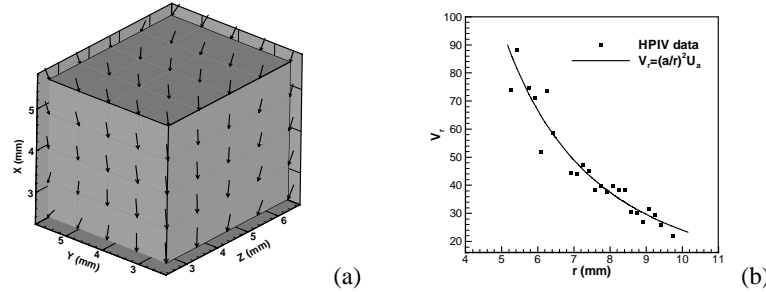


Fig. 8. Digital HPIV results of the simulated flow around a collapsing 2mm spherical cavity centered at (0, 0, 0). (a) 3D vector map. (b) Comparison between the measured radial velocity V_r and its theoretical solution.

(b) Application to a laboratory particle suspension

The digital in-line holography system was also tested by a laboratory particle suspension with random distribution. In the experiment, 50 μm particles (Dantec PSP-50) were seeded in a small Plexiglas tank of 70 mm in depth. A 532 nm collimated laser beam passed through the tank and hit on a 12-bit CCD sensor ($8.58 \times 6.86 \text{ mm}^2$). The recorded in-line holograms were transferred to a PC and processed by the data processing software described before. Fig. 9 shows an example of the particle hologram. There are totally about 500 particles in this hologram, corresponding to a particle number density $n_p = 0.125 \text{ mm}^{-3}$.

Particle 3D positions were extracted from the digital holograms. The two-particle radial distribution function (RDF) was calculated using the formula given by Reade and Collins (2000). Fig. 10 shows the results obtained from two holograms. It is seen that the RDF peaks at about $r=2$ mm. This distance is actually the distance between two neighbor particles in a nominally uniform suspension with $n_p = 0.125 \text{ mm}^{-3}$.

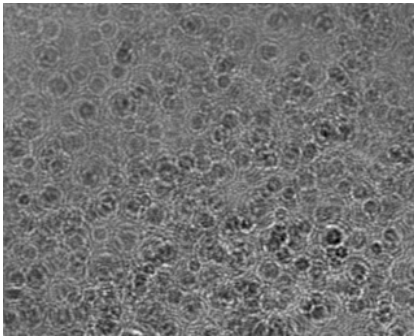


Fig. 9. Digitally recorded in-line hologram of 50 μm particles with $n_s = 0.125 \text{ mm}^{-3}$.

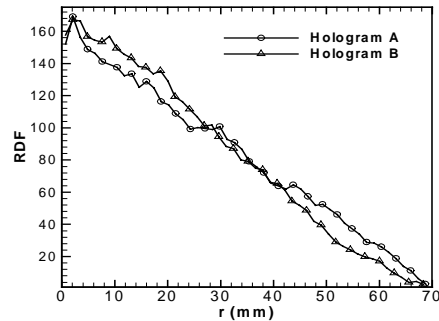


Fig. 10. Two-particle radial distribution function (RDF) obtained from two holograms.

7 Summary

In this paper, we have described a digital in-line holography system for particulate flow diagnostics. This system records in-line holograms directly to a CCD camera and reconstructs them numerically. A novel particle extraction method, which uses complex amplitude of the reconstructed wave, has been developed for this system. With the addition of Concise Cross Correlation (CCC) and particle pairing method (Pu and Meng 2000), this system works as a digital holographic particle image velocimetry (HPIV) system, which measures 3D velocity of individual particles. This system has been tested by simulated particle holograms at several particle number densities to check the

accuracies of both position and velocity measurement. The system has also been applied to measuring a laboratory particle suspension and gave the correct two-particle radial distribution function.

References

- Adams M; Kreis T; Juptner W** (1997) Particle size and position measurement with digital holography. Proc. SPIE, 3098, 234-240
- Boyer K; Solem JC; Longworth JW; Borisov AB; Rhodes CK** (1996) Biomedical three-dimensional holographic microimaging at visible, ultraviolet and X-ray wavelength. Nat. Med. (N.Y.), 2, 939-941
- Goodman JW; Lawrence RW** (1967) Digital image formation from electronically detected holograms. Appl. Phys. Lett., 11, 77-79
- Kreis T; Adams M; Juptner W** (1999) Digital in-line holography in particle measurement. Proc. SPIE, 3744, 54-64
- Lighthill J** (1986) An informal introduction to theoretical fluid mechanics. Oxford Univ. Press, 104
- Meng H; Anderson WL; Hussain F; Liu D** (1993) Intrinsic speckle noise in in-line particle holography. J. Opt. Soc. of Amer. A, 10, 2046-2058
- Meng H; Hussain F** (1995) In-line recording and off-axis viewing technique for holographic particle velocimetry. Appl. Opt. 34, 1827-1840
- Murata S; Yasuda N** (2000) Potential of digital holography in particle measurement. Opt. & Laser Tech., 32, 567-574
- Nishihara K; Hatano S; Nagayama K** (1997) New method of obtaining particle diameter by the fast Fourier transform pattern of the in-line hologram. Opt. Eng., 36, 2429-2439
- Onural L; Scott PD** (1987) Digital decoding of in-line holograms. Opt. Eng. 26, 1124-1132
- Owen RB; Zozulya AA** (2000) In-line digital holographic sensor for monitoring and characterizing marine particulates. Opt. Eng. 39, 2187-2197
- Pan G; Meng H** (2001) Particle extraction from digital in-line holograms using complex amplitude. in preparation
- Pu Y; Meng H** (2000) An advanced off-axis holographic particle image velocimetry (HPIV) system. Exp. Fluids, 29, 184-197
- Pu Y; Song X; Meng H** (2000) Off-axis holographic particle image velocimetry for diagnosing particulate flows. Exp. Fluids, S, S117-S128
- Reade WC; Collins LR** (2000) Effect of preferential concentration on turbulent collision rates. Phys. Fluids, 12, 2530-2540
- Schedin S; Pedrini G; Tiziani HJ; Mendoza Santoyo F** (1999) Simultaneous three-dimensional dynamic deformation measurements with pulsed digital holography. Appl. Opt., 38, 7056-7062
- Schnars U; Juptner W** (1994) Direct recording of holograms by a CCD target and numerical reconstruction. Appl. Opt., 33, 179-181
- Thompson BJ** (1963) Diffraction by opaque and transparent particles. J. SPIE, 2, 43-46
- Trolinger JD; Beltz RA; Farmer WM** (1969) Holographic techniques for the study of dynamic particle fields. Appl. Opt., 8, 957-961
- Yaroslavskii LP; Merzlyakov NS** (1980) Methods of digital holography. Consultants Bureau, New York
- Zhang T; Yamahuchi I** (1998) Three-dimensional microscopy with phase-shifting digital holography. Opt. Lett., 23, 1221-1223